# Genesis of syntectonic hydrothermal veins in the igneous rock of teschenite association (Outer Western Carpathians, Czech Republic): growth mechanism and origin of fluids

TOMÁŠ URUBEK[1,✉,2], ZDENĚK DOLNÍČEK[2] and KAMIL KROPÁČ[2]

[1]Department of Geological Sciences, Faculty of Science, Masaryk University, Kotlářská 2, 611 37 Brno, Czech Republic;
✉urubek.tomas@seznam.cz
[2]Department of Geology, Palacký University, Tř. 17. listopadu 12, 771 46 Olomouc, Czech Republic;
zdenek.dolnicek@upol.cz; kamil.kropac@upol.cz

**Abstract:** Hydrothermal mineralization hosted by the Lower Cretaceous igneous rock of the teschenite association at Jasenice (Silesian Unit, Flysch Belt, Outer Western Carpathians) occurs in two morphological types — irregular vein filled by granular calcite and regular composite vein formed by both fibrous and granular calcite and minor chlorite, quartz, and pyrite. Crosscutting evidence indicates that the granular veins are younger than the composite vein. The composite vein was formed by two mechanisms at different times. The arrangement of solid inclusions in the marginal fibrous zone suggests an episodic growth by the crack-seal mechanism during syntectonic deformation which was at least partially driven by tectonic suction pump during some stages of the Alpine Orogeny. Both the central part of the composite vein and monomineral veins developed in a brittle regime. In these cases, the textures of vein suggest the flow of fluids along an open fracture. The parent fluids of both types of vein are characterized by low temperatures (Th = 66–163 °C), low salinities (0.4 to 3.4 wt. % NaCl eq.), low content of strong REE-complexing ligands, and $\delta^{18}$O and $\delta^{13}$C ranges of +0.2/+12.5 ‰ SMOW and –11.8/–14.1 ‰ PDB, respectively. The parent fluids are interpreted as the results of mixing of residual seawater and diagenetic waters produced by dewatering of clay minerals in the associated flysch sediments. The flow of fluids was controlled by tectonic deformation of the host rock.

**Key words:** Outer Western Carpathians, teschenites, syntectonic vein, fluid inclusions, stable isotopes, REE.

## Introduction

Different types of mineralogically distinct hydrothermal veins occur in all levels of the Earth's crust. Their morphology, texture, mineral composition, and chemistry offer valuable information about geological processes. In particular, veins are useful to unravel the deformation history of host rocks (Ramsay & Huber 1983; Bons & Montenari 2005). The study of the shape and spatial orientation of veins can help to determine the paleostrain orientation, while fluid inclusions record the composition, pressure, and temperature of vein-forming fluids. A detailed description of internal vein microstructure refining the paleostress analysis of veins presents an important part of investigation of hydrothermal veins. Especially fibrous veins can record the opening trajectories of veins in greater detail (Hilgers & Sindern 2005).

The hydrothermal mineralization in the Silesian unit was studied recently from the mineralogical and genetic points of view using fluid inclusion microthermometry, stable isotopes, and trace elements (Urubek 2006, 2009; Polách 2008; Polách et al. 2008; Urubek & Dolníček 2008; Urubek et al. 2009; Dolníček et al. 2010a,b, 2012). The results of previous research indicate that the mineralogically most interesting mineral associations occur in igneous rocks of the teschenite association. Mineral assemblages involve mainly carbonates, chlorite, quartz, opal, chalcedony, and rare zeolites or sulphides. These post-magmatic mineral associations were

formed from low-temperature (< 50 to 220 °C) and low-salinity (0.0 to 4.5 wt. % NaCl equiv.) fluids with elevated $\delta^{18}$O values (+2 to +14 ‰ SMOW). The parent fluids are interpreted as a mixture of magmatic waters (remaining after crystallization of magma), diagenetic waters (produced by thermal alteration of clay minerals in clastic sediments) and seawater.

This contribution focuses on the genesis of a fibrous vein hosted by magmatic rock of the teschenite association found at Jasenice. The microstructure, stable isotope, fluid inclusion and trace element studies of vein minerals provided pilot information about the physico-chemical conditions of formation of syntectonic hydrothermal veins. Unlike the Polish and Slovak parts of the Western Carpathians (Świerczewska et al. 2000; Milovský et al. 2003; Milovský & Hurai 2003), essentially nothing is known about syntectonic veining in the Czech (i.e. westernmost) segment of the Western Carpathians.

## Geological setting and studied site

The Carpathians are a part of the European Alpine chain created by convergence and collision of the European and African plates (Golonka et al. 2000). In the NE part of the Czech Republic, the Outer Carpathians form a NW-verging fold-and-thrust belt composed largely of Upper Jurassic-to-Upper Oligocene flysch arranged into several nappes — Subsilesian, Silesian and Magura Nappes, listed from tectonic
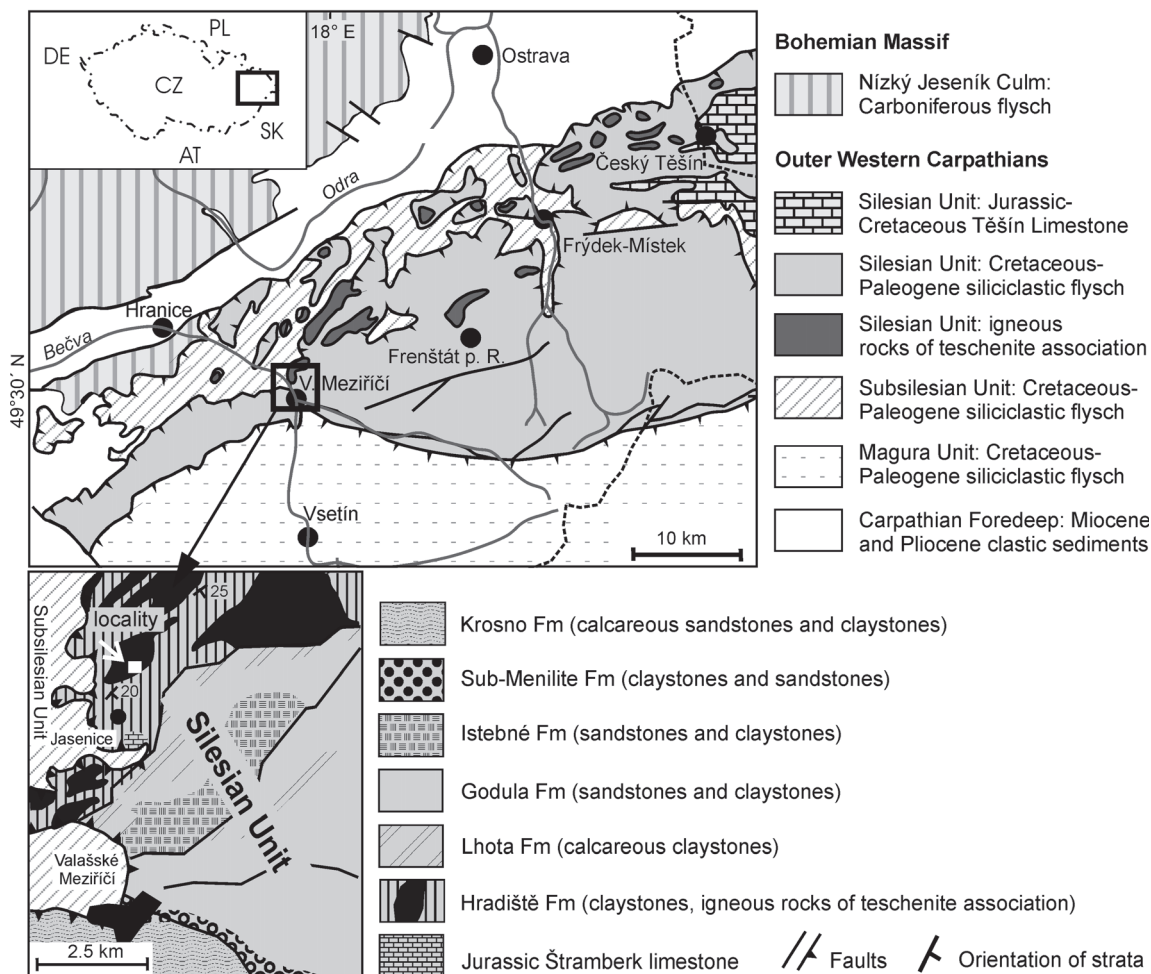
**Fig. 1.** Geological position of the Jasenice locality in the Outer Western Carpathians flysch nappe system.

foot-wall to hanging-wall (Fig. 1). The studied locality is situated in the Godula Development of the Silesian Unit which consists mainly of Upper Jurassic-to-Upper Oligocene marine sedimentary rocks (Eliáš 1970; Stráník et al. 1993). The basal calcareous turbidites (Cieszyn limestones of the Late Jurassic age) are followed by black calcareous shales alternating with thin layers of sandstones (Hradiště Formation) passing upwards into black silicified shales (Veřovice Formation). Pelocarbonate (mainly siderite) horizons in claystone-rich cycles occur in some places. The subsidence and spreading during the Lower Cretaceous was accompanied by the extrusion of basic lavas giving rise to teschenites. In the period from the Late Turonian to Early Eocene the sedimentation of thick bedded coarse grained turbidites and fluxoturbidites (Godula Beds, Istebna Beds) took place. This period of intense turbiditic sedimentation was generally connected with Laramian tectonic movements that caused uplift of the source areas associated with erosion and redeposition of clastic sediments. The Oligocene sequences are characterized by the presence of layers of dark organic-rich biogenic silicite (Menilite formation). The shortening events related to the Alpine Orogeny started in the Paleocene and continued up to the early Late Miocene (Plašienka et al. 1997). During these tectonic phases the whole sedimentary sequence including the

magmatic rocks was folded and thrusted towards the NW onto the SE part Bohemian Massif.

The mafic quartz-free alkaline-to-subalkaline igneous rocks of the teschenite association are products of a submarine Early Cretaceous (Hauterivian–Barremian) magmatism. They form hypoabyssal sills, submarine extrusions and pillow lavas and are widespread in the area between Hranice in Moravia and Bielsko-Biała in Poland. Rocks of the teschenite association are characterized by wide variability in textures, mineral composition, and geochemistry (Pacák 1926; Šmíd 1962; Kudělásková 1987; Hovorka & Spišiak 1988; Dostal & Owen 1998; Lucińska-Anczkiewicz et al. 2002; Spišiak & Mikuš 2008). Petrographically, they include teschenites, picrites, alkaline basalts, and monchiquites (Šmíd 1962).

The studied hydrothermal mineralization was found in coarse-grained black-green massive picrite (Urubek 2009) which forms a small natural outcrop (2×1 m) in the bed of an unnamed brook, about 1 km east from the center of the village of Jasenice near Valašské Meziříčí (N 49°32.653′ E 17°57.803′, altitude 592 m a.s.l.). Throughout the whole outcrop, the picrite is strongly altered. In thin section the amygdaloid texture is observed with up to 3 mm large amygdules filled by calcite and chlorite. The rock also contains phenocrysts of olivine, which is partially replaced by serpen-

tine and calcite. Brown amphibole, laths of plagioclase, and flakes of biotite (which is often chloritized) constitute the rock matrix.

## Methods

The WDX electron microprobe analyses of minerals were performed using Cameca SX-100 microprobe at the Masaryk University in Brno. For carbonate and silicate minerals the accelerating voltage of 15 kV, 20 nA beam current and beam diameter of 10 μm (carbonates) and 5 μm (phyllosilicates), respectively, have been used (Dolníček et al. 2010b; Kropáč et al. 2012).

Fluid inclusions were investigated by means of petrography and microthermometry in standard doubly polished wafers and cleavage fragments. The distinguishing of primary (P), and secondary (S) inclusions was done according the criteria given by Roedder (1984) and Shepherd et al. (1985). Microthermometric parameters were measured using the Linkam THMSG 600 stage at the Palacký University, Olomouc. The temperature of final homogenization (Th) and melting temperature of ice (Tm ice) were measured. The stage was calibrated with inorganic standards and synthetic fluid inclusions. The reproducibility is within 0.1 °C for temperatures between –56.6 and 0 °C, and within 1 °C for the temperature of 374.1 °C. The isochores were calculated using the computer program Flincor (Brown 1989) with the equation of state by Zhang & Frantz (1987).

For bulk chemical analyses, the carbonate samples weighing between 1 and 2 g were hand picked under a binocular microscope and then pulverized in the agate mortar. The host rock was powdered in an epicyclic mill and reduced in weight by quartering. The chemical analyses were performed in the ACME Analytical Laboratories, Vancouver, Canada. Aliquots for analyses of the heavy metals were dissolved in hot (95 °C) aqua regia and analysed using the ICP-ES method. Other determined elements including refractory metals and rare earth elements (REE) were analysed by ICP-MS in another sample aliquot, which was decomposed using $LiBO_2$ fusion followed by leaching in diluted (5%) $HNO_3$. Reproducibility of the results is within 5–10 % based on analyses of standards. The REE concentrations were normalized to C1-chondrite according to values determined by Anders & Grevesse (1989). The Ce, Eu, and Yb anomalies were calculated using the following equations (McLennan 1989; Monecke et al. 2002): $Ce/Ce* = Ce_N/\sqrt{(La_N*Pr_N)}$, $Eu/Eu* = Eu_N/\sqrt{(Sm_N*Gd_N)}$, $Yb/Yb* = Yb_N/\sqrt{(Tm_N*Lu_N)}$.

Stable isotope analyses were conducted in the laboratories of the Czech Geological Survey, Prague, using a Finnigan MAT 251 mass spectrometer. The conversion of carbonates to $CO_2$ was done by reaction with 100% orthophosphoric acid (McCrea 1950). The results of isotope analyses are conventionally expressed in delta (δ) notation as per mil (‰) deviation from commonly used standards (PDB, SMOW). Uncertainty is better than ±0.05 and ±0.1 for $δ^{13}C$ and $δ^{18}O$, respectively. The isotopic composition of the parent fluid was calculated using the equations published by O'Neil et al. (1969) and Deines et al. (1974).

## Results

### Vein types

Two types of vein texture were distinguished at the studied locality: granular (V1) and composite (V2). Based on cross-cutting evidence the V1 veins are younger than the V2 vein.

### Granular veins (V1)

The outcrop is cut by seven hydrothermal veins 2 and 8 mm thick and up to several meters in length. A preferential orientation of veins was not observed: they strike SW–NE, SSW–NNE, and NNW–SSE and are steeply (60–80°) dipping to NW, WNW, and WSW, respectively (Fig. 2). The tectonic striae have never been observed in the vein fill or on the contact of the rock and vein. No remnants of host rock occur within the vein.

Granular veins are composed only of white calcite. In thin section, the calcite grains are anhedral and slightly elongated perpendicularly to the course of veins. The sizes of grains are variable, ranging from 0.25 mm (marginal parts of veins) up to 1 mm (center of veins). The undeformed (i.e. straight) twinning lamellae have been sporadically observed in the calcite grains.

### Composite vein (V2)

Two composite extensional veins are undeformed and their thickness ranges from 5 to 20 mm. The veins strike NNW–SSE (dip ca. 20° to WSW) (Fig. 2) and are composed of calcite, chlorite, quartz, and sporadic pyrite. The internal fabric corresponds to the composite unitaxial syntaxial type
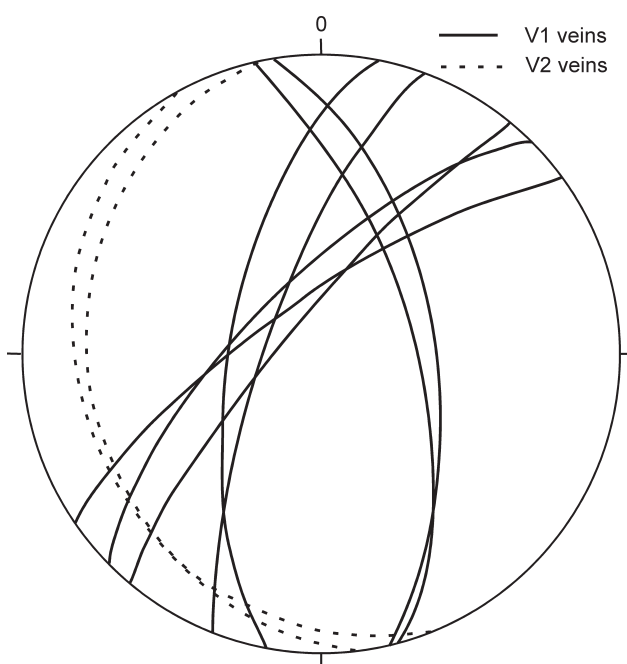


**Fig. 2.** The arc diagram of hydrothermal veins at the locality Jasenice. Lower hemisphere of the Lambert's projection.
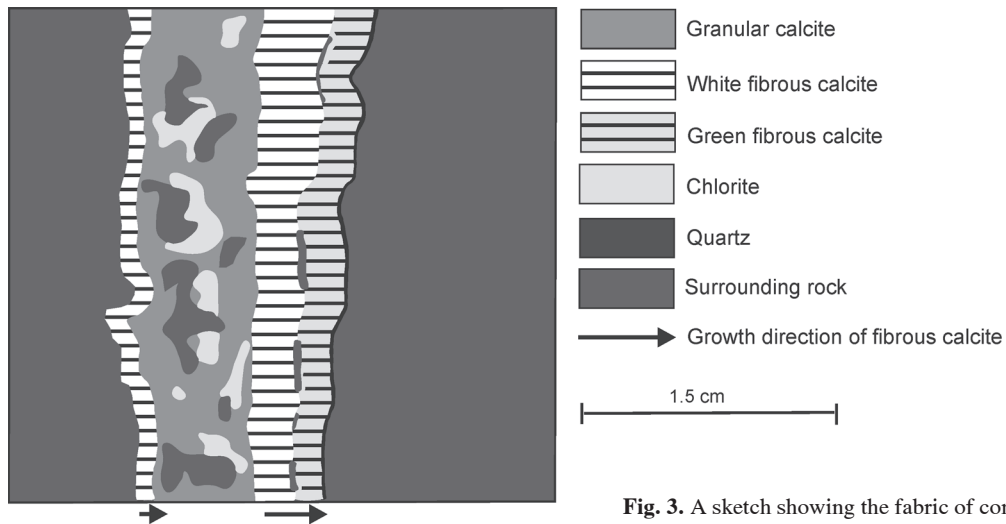
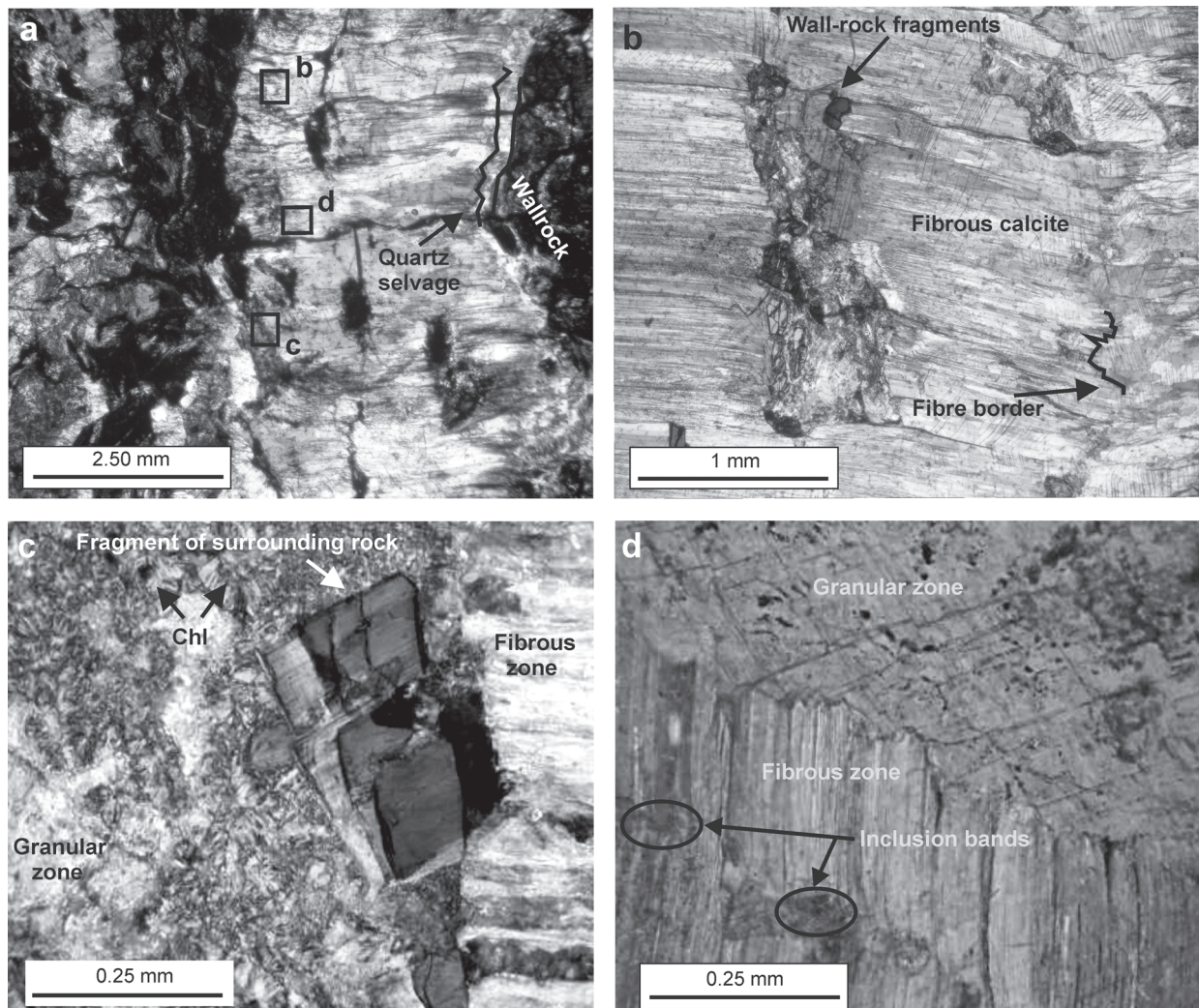**Fig. 3.** A sketch showing the fabric of composite syntectonic vein.



**Fig. 4.** Textural features and mineral paragenesis of hydrothermal mineralization from Jasenice in thin sections. **a** — Composite vein with uni-taxial fibrous part (right) where fibres grew from the center of the vein towards the wall-rock. The wall rock surface is lined by a thin rim of quartz crystals that grew from the wall rock into the vein; **b** — Enlargement of rectangle in (a) showing the fibrous zone in detail; **c–d** — En-largement of rectangle in (a) showing the interface between granular and fibrous calcite in syntectonic vein. Cc — calcite, Chl — chlorite; fan-shaped aggregate closed in the granular calcite. All pictures were made in transmitted light and crossed polars.
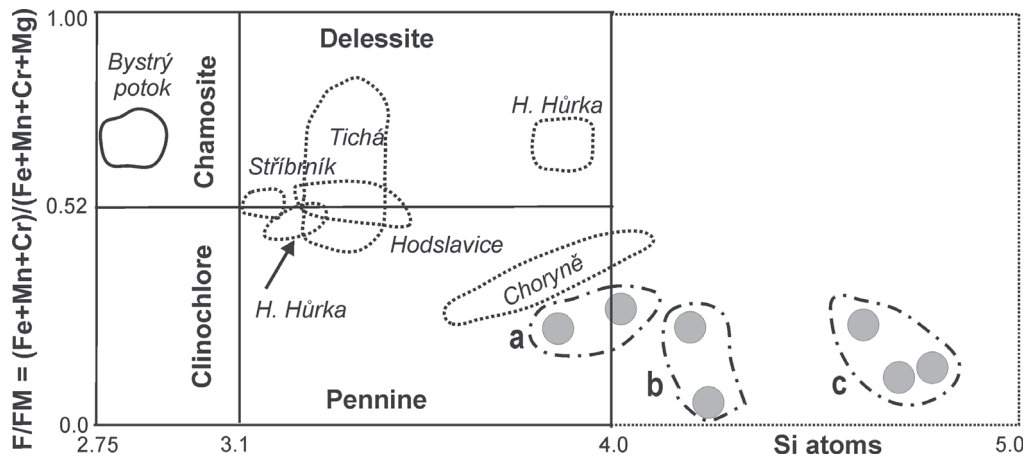
**Fig. 5.** Classification of chlorite from Jasenice (data points) in the diagram by Melka (1965) and a comparison with other mineralizations in the Silesian Unit (outlined) hosted by both teschenite rock series (dashed line) and flysch sediments (full line). The comparative data are from Urubek & Dolníček (2008), Dolníček & Polách (2009), Urubek et al. (2009), Dolníček et al. (2010a,b, 2012). **a** — chlorites from matrix of igneous rock; **b** — chlorites from fibrous zone of composite vein; **c** — chlorites from granular zone of composite vein.

of fibrous veins (Ramsay & Huber 1983; Passchier & Trouw 1996) composed of a central part (median) and peripheral fibrous parts. The median has a constant thickness of about 10 mm and is formed by fine-grained white to light brown calcite containing fragments of surrounding rock. These fragments are situated mainly at the edge of the central part of the vein. The marginal part adjacent to the host rock is characterized by development of fibrous calcite, which shows the distinct growth zonality. The growth zones differ in colour, which is milky white, light green or grey (Fig. 3).

Microscopic study demonstrates that *calcite* is the dominant mineral phase. It completely fills the central part of the vein (median) in the form of isometric anhedral grains. The sizes of grains vary from 1.2 mm up to 3.7 mm. In the marginal parts calcite forms fibres arranged perpendicularly to the walls of the vein. Calcite fibres are slightly curved near the median line. The thickness of individual fibres ranges from 20 µm to about 0.5 mm, with a distinct increase of the thickness towards the vein-rock interface. In the case of greater thickness of fibres the twinning lamellae showing no deformation are observed. The growth zoning of fibrous calcite is sometimes highlighted by the presence of fragments of surrounding rocks (columns of brown amphibole and flakes of chloritized biotite) and between the growing fibres the toothy border is observed. Fragments of host rock are much larger than the fibre diameter and are arranged as inclusion bands parallel to the vein margin. In the pressure shadows behind these rock fragments, calcite aggregates formed by isometric grains are developed. The wall rock fragments are sometimes present on boundaries between fibres of calcite. At the interface between the vein filling and the surrounding rock narrow quartz selvage was found, consisting of small anhedral quartz crystals that grew out from the wall rock. The width of this selvage is quite constant (about 0.5 mm) and independent of that of the vein (Fig. 4a).

The EPMA analyses show that all the vein carbonate is calcite. Chemical composition of fibrous calcite is very simple, showing up to 1.0 wt. % MgO, FeO or MnO. The calcite located near the median has in addition an elevated content of Mn (1.3 wt. % MnO).

*Chlorite* has been detected both in the median and in the fibrous periphery of the vein. Chlorite of the median typically forms fan-shaped aggregates (Fig. 4c) composed of fine (100–200 µm) flakes. Chlorite is weakly pleochroic (light yellow–light brown-yellow) and shows anomalous interference colours in green hues. The occurrence of these aggregates is associated mainly with the fragments of the surrounding rock.

Chlorite in association with fibrous calcite forms elongated individuals (ca. 100 µm in long), which are arranged parallel to calcite fibres and exhibit both distinct pleochroism (colourless — light green) and anomalous interference colours in green hues. Chlorite is typically associated with one of the growth zones, which has macroscopically green colour. Electron microprobe analyses were collected from chlorites hosted in granular and fibrous calcite, and from those from the host rock. According to Melka's classification (1965), all the analysed chlorites belong to the pennine: Si = 3.89 to 4.78 apfu, Fe/(Fe + Mg) = 0.04–0.26 (Fig. 5).

The occurrence of *pyrite* is restricted only to the central part of the vein, where it is enclosed by calcite. Pyrite forms subhedral to anhedral isolated grains about 0.5 mm in size, occurring in the form of hemispherical aggregates in the proximity of fragments of surrounding rock. The solitary pyrites sometimes exhibit growth zonality characterized by higher porosity in some incremental zones.

*Quartz* overgrows the walls of the vein where it forms the selvage of almost constant thickness (see above) composed of anhedral grains. Grains of quartz up to 0.5 mm large show no evidence of fracturing but exhibit undulatory extinction.

### Fluid inclusions

Fluid inclusions suitable for microthermometric analysis were found in both V1 and V2 veins. In the case of V2 several subsamples were taken: from the median (granular calcite I),

peripheral fibrous parts: white (calcite II), greenish (calcite III), calcite associated with quartz selvage from fibrous growth zones (calcite IV); and calcite from the mononineral granular — V1 vein (calcite V).

Calcites contain abundant primary and secondary fluid inclusions showing equant shapes and sizes ranging between 2 and 6 µm. The fluid inclusions are distributed relatively uniformly in the studied samples. The observed primary and secondary inclusions are one-phase (L-only). Two-phase (L+V) inclusions with essentially constant liquid-vapour ra-

tios (gaseous phase takes ca. 5 vol. %) are less frequent. An exception is calcite V which contains mainly L+V and less one-phase L inclusions. Most primary inclusions are solitary, show regular rounded shapes, sporadically they are slightly elongated along twinning lamellae. The secondary fluid inclusions are arranged along healed microfractures. The homogenization temperatures of primary fluid inclusions from calcite I and calcite V are characterized by slightly lower values (66–142 °C) than in the cases of calcite II, III, and IV (103–163 °C). Generally, secondary inclusions showed lower homogenization temperatures (about 100 °C). Fluid inclusions have generally similar cryometric parameters. In all cases, the inclusions freeze at temperatures from –34 to –43 °C. The last ice melts at temperatures between –0.2 and –2.0 °C (Fig. 6a) indicating bulk fluid salinities between 0.4 and 3.4 wt. % NaCl eq. (Bodnar 1993) (Table 1). The cryometric data of one-phase inclusions were measured after heating to a temperature exceeding 220 °C which led to stretching of inclusions and subsequent bubble nucleation. The secondary inclusions have generally similar microthermometric parameters as the primary ones (Table 1).

The predominance of one-phase aqueous inclusions could indicate very low trapping temperatures (below 50 °C) (Goldstein & Reynolds 1994), however, this is not in accordance with homogenization temperatures of two-phase inclusions ranging between 66 and 163 °C (Table 1). The absence of vapour bubbles is often observed in smaller (<5 µm) inclusions implying that metastability of the phase composition of the fluid inclusions could play a role.

There are no systematic differences between L-only and L+V inclusions in their cryometric parameters, which further support the idea about a metastable nature of the liquid inclusions. The eutectic temperature was impossible to measure due to the small size of the inclusions.

### Stable isotopes

The samples of carbonate were analysed for carbon and oxygen isotope compositions from both V1 and V2 veins (Table 2). $\delta^{18}O$ values varying between –9.9 and –11.2 ‰ PDB and $\delta^{13}C$ values between –12.5 and –11.5 ‰ PDB were determined in the fibrous calcite of V2 vein. The granular calcite from the median of V2 vein showed the $\delta^{18}O$ value of –4.5 ‰ PDB and the $\delta^{13}C$ value of
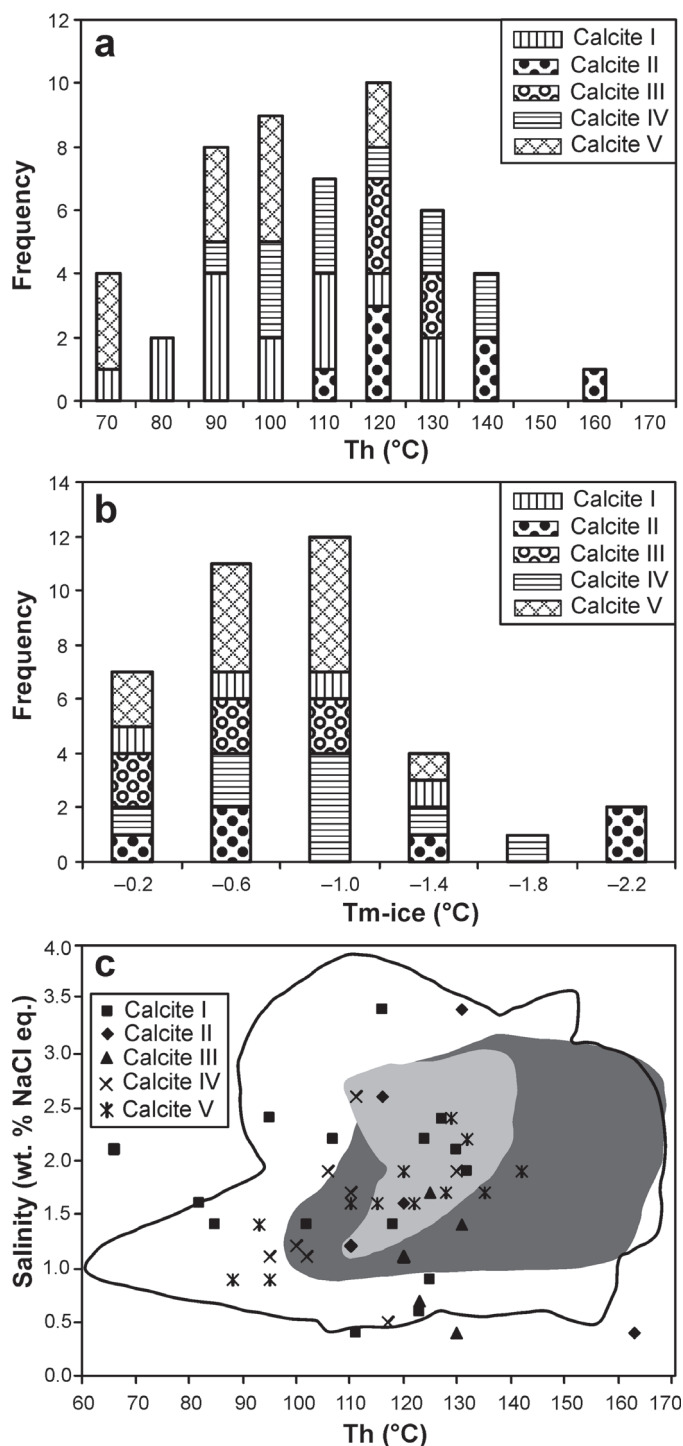


Fig. 6. Results of microthermometry of primary fluid inclusions from Jasenice. **a** — Histogram of homogenization temperatures of L+V inclusions; **b** — Histogram of melting temperatures of last ice; **c** — Th-salinity plot. The comparative data (**white field** — vein carbonates cutting magmatic rocks in the Silesian Unit; **light grey field** — diagenetic veins hosted by sedimentary rocks in the Silesian Unit; **dark grey field** — post-tectonic veins hosted by sedimentary rocks in the Silesian Unit) are from Świerczewska et al. (2000), Polách (2008), Polách et al. (2008), Urubek & Dolníček (2008, 2011), Dolníček & Polách (2009), Urubek (2009), Dolníček et al. (2010a,b, 2012), and Jarmolowicz-Szulc et al. (2012).

**Table 1:** Results of fluid inclusion microthermometry.

| Sample | FI type | Phase composition | Th (L+V) (°C) | Tf (°C) | Tm ice (°C) | Salinity (wt. % NaCl eq.) |
|---|---|---|---|---|---|---|
| **Calcite I** | P | L, rarely L+V | 66–135 | –39/–43 | –0.2/–1.4 | 0.4–2.4 |
| | S | | 75–90 | –38/–41 | –0.4/–0.8 | 0.7–1.4 |
| **Calcite II** | P | L, rarely L+V | 110–163 | –37/–41 | –0.2/–2.0 | 0.4–3.4 |
| **Calcite III** | P | L, rarely L+V | 120–131 | –38/–40 | –0.2/–0.9 | 0.4–1.6 |
| | S | L | n.a. | –36/–42 | –0.4/–0.6 | 0.7–1.1 |
| **Calcite IV** | P | L, rarely L+V | 103–148 | –39/–41 | –0.3/–1.5 | 0.5–2.6 |
| | S | L, L+V | 110–125 | –39/–42 | –0.5/–1.4 | 0.9–2.4 |
| **Calcite V** | P | L+V, rarely L | 88–142 | –34/–38 | –0.5/–1.4 | 0.9–2.4 |
| | S | L, rarely L+V | 93–115 | –36/–39 | –0.5/–0.9 | 0.9–1.6 |

**P** — primary fluid inclusions, **S** — secondary fluid inclusions, **L** — monophase liquid fluid inclusions, **L+V** — liquid–rich two phase fluid inclusions (V — vapour phase), **n.a.** — not applicable.

**Table 2:** Carbon and oxygen isotope composition of calcites and $\delta^{13}C$ and $\delta^{18}O$ values of their parent fluids calculated for the given temperature.

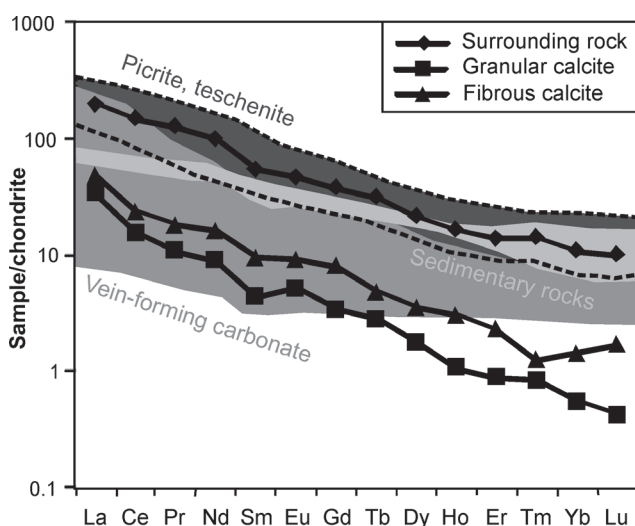| | Mineral | | | | Hydrothermal solution | |
|---|---|---|---|---|---|---|
| Sample | $\delta^{13}C$ ‰ (PDB) | $\delta^{18}O$ ‰ (PDB) | $\delta^{18}O$ ‰ (SMOW) | T (°C) | $\delta^{18}O$ ‰ (SMOW) | $\delta^{13}C$ ‰ (PDB) |
| **Calcite I** | –10.3 | –4.5 | 26.3 | 66/135 | 5.0/12.5 | –12.1/–11.8 |
| **Calcite II** | –12.5 | –9.9 | 20.7 | 110/163 | 4.6/9.0 | –14.1/–13.9 |
| **Calcite III** | –11.5 | –11.2 | 19.4 | 95/135 | 1.7/5.6 | –13.1/–13.0 |
| **Calcite V** | –11.4 | –10.9 | 19.6 | 80/110 | 0.2/3.4 | –13.1/–12.7 |



**Fig. 7.** REE chondrite-normalized patterns of hydrothermal calcites and host magmatic rock. Normalization values are from Anders & Grevesse (1989). The comparative data from other localities in the Silesian Unit studied by Polách (2008), Polách et al. (2008), Urubek & Dolníček (2008, 2011), Dolníček & Polách (2009), Urubek (2009), and Dolníček et al. (2010a,b, 2012), are visualized as shaded fields.

–10.3 ‰ PDB. One calcite from granular vein (V1) intersecting the composite vein yielded the $\delta^{18}O$ value of –10.9 ‰ PDB and the $\delta^{13}C$ value of –11.4 ‰ PDB (Table 2).

### Trace elements

The calcites from both the middle and margin of composite vein and one sample of host rock have been analysed for selected trace elements (Table 3). The calcites from the composite vein show increased Sr contents (983 and 1100 ppm) which are slightly enriched in comparison with host rock

(845 ppm). Both samples show significantly lower contents (31 and 72 ppm) of Ba in comparison with surrounding rock (706 ppm).

The concentrations of rare earth elements (REE) are lower in the calcite ($\Sigma REE = 25$ ppm) than in the host picrite ($\Sigma REE = 221$ ppm). The chondrite-normalized patterns (Fig. 7) follow similar trends in all samples characterized by systematic decrease from La to Lu (LREE-enriched pattern). Granular calcite from median exhibits a weak positive Eu anomaly (Eu/Eu* = 1.35) whereas other samples are without Eu anomaly. All samples show weak negative Ce anomalies (Ce/Ce* = 0.61–0.63).

## Discussion

### The growth mechanism

The texture of younger V1 veins suggests the transport of fluid along an open fracture resulting in a blocky vein microstructure combined with a decrease of growth rate and increase of the grain size towards the center of the vein (Hilgers et al. 2004; Hilgers & Sindern 2005). The observed orientation of veins corresponds to the major system of faults in this area that formed during the Late Miocene (Fig. 1) (Stráník et al. 1993).

The regular course of older composite V2 vein suggests that the vein formation was initiated by brittle fracturing of rock (Cosgrove 1993; Hilgers & Sindern 2005). The tension veins initially formed parallel to the maximum shortening direction which corresponds to the direction of the vein (Bons 2000). The formation of the regional folds in the Outer Carpathians commenced under horizontal compression (Szczesny 2003), which corresponds to a low angle of dip of the vein. In addition, the axis of the largest stress ($\sigma_1$) was perpendicular to the fold axes and the smallest stress axis

**Table 3:** Trace element abundances in calcite and host rock samples from Jasenice. All values are in ppm except for Au in ppb.

| Sample | Calcite I | Calcites II-IV | Host rock |
|--------|-----------|----------------|-----------|
| **Ba** | 30.8 | 72 | 706 |
| **Be** | <1.0 | <1 | 1 |
| **Co** | 1.0 | 4.1 | 55 |
| **Cs** | 0.1 | <0.1 | 0.2 |
| **Ga** | <0.5 | 1.6 | 16.4 |
| **Hf** | <0.5 | <0.1 | 6.3 |
| **Nb** | <0.5 | 2.7 | 81 |
| **Rb** | <0.5 | <0.1 | 13.7 |
| **Sn** | <1.0 | <1 | 2 |
| **Sr** | 983 | 1100 | 845 |
| **Ta** | <0.1 | <0.1 | 4.3 |
| **Th** | 0.1 | 0.3 | 6.4 |
| **U** | 0.2 | 0.4 | 2.2 |
| **V** | <5.0 | <8 | 237 |
| **W** | 0.1 | 0.5 | <0.5 |
| **Zr** | <0.5 | 11.4 | 255 |
| **Y** | 2.4 | 4.6 | 26.5 |
| **Mo** | <0.1 | | 1.2 |
| **Cu** | 1.5 | | 43.7 |
| **Pb** | 0.9 | | 4.3 |
| **Zn** | 19 | | 87 |
| **Ni** | 10 | | 170.8 |
| **As** | <0.5 | | 1.4 |
| **Cd** | <0.1 | | 0.1 |
| **Sb** | <0.1 | | <0.1 |
| **Bi** | <0.1 | | <0.1 |
| **Ag** | <0.1 | | <0.1 |
| **Au** | <0.5 | | <0.5 |
| **Hg** | 0.01 | | <0.01 |
| **Tl** | <0.1 | | <0.1 |
| **Se** | 0.5 | | <0.5 |
| **La** | 7.9 | 11.3 | 46.2 |
| **Ce** | 9.3 | 14.2 | 89 |
| **Pr** | 0.96 | 1.60 | 11.24 |
| **Nd** | 4 | 7.3 | 44.9 |
| **Sm** | 0.64 | 1.38 | 8.02 |
| **Eu** | 0.29 | 0.51 | 2.62 |
| **Gd** | 0.67 | 1.57 | 7.41 |
| **Tb** | 0.1 | 0.17 | 1.12 |
| **Dy** | 0.43 | 0.85 | 5.18 |
| **Ho** | 0.06 | 0.17 | 0.91 |
| **Er** | 0.14 | 0.36 | 2.21 |
| **Tm** | 0.02 | 0.03 | 0.34 |
| **Yb** | 0.09 | 0.23 | 1.77 |
| **Lu** | 0.01 | 0.04 | 0.24 |
| **Σ REE** | 24.61 | 39.71 | 221.16 |
| **Yb/Yb*** | 0.90 | 1.01 | 0.85 |
| **Eu/Eu*** | 1.35 | 1.05 | 1.03 |
| **Ce/Ce*** | 0.61 | 0.63 | 0.91 |

**Calcite I** — granular calcite from V2 vein, **Calcites II–IV** — fibrous calcite from V2 vein.

($\sigma_3$) retained a vertical position (Szczesny 2003). Moreover, the direction of the V2 vein corresponds to the first event of the tectonic evolution of the Outer Carpathians when the folding and thrusting were propagated to the NNW in the study area (Botor 2006) and gave rise to the NNW-verging folds and thrusts in the flysch rocks (Fig. 1). The compression in the NNW-direction caused movement of the Silesian Unit in the Czech segment (Födör 1991; Havíř 2000; Mlynář 2000). The difference between the texture of the median zone and fibrous margin of the V2 vein indicates distinctly different growth mechanisms for the two parts of the tension vein.

*The fibrous calcite.* On the basis of linear bands of solid inclusions parallel to the vein wall, Ramsay (1980) proposed a process of repeated fracturing and sealing — the so-called crack-seal mechanism. The regular textural periodicity suggests veining induced by hydraulic fracturing under cyclic changes in pore pressure. These crack-seal veins display sawtooth shaped grain boundaries between adjacent elongated grains with preferred growth of favourably oriented crystals. Solid inclusions will be incorporated when a fracture reopens after crack collapse and re-sealing. This happens if the fluid pressure increases to values larger than the minimum principal stress oriented perpendicularly to the fracture wall and the tensile strength of the rock. Under such conditions, crystals will grow until fluid pressure drops due to fracturing and the void collapses (crack-seal mechanism with incremental growth). This may result in a feedback system, where the discharge seals off the fluid pathways and fluid pressure repeatedly increases until the rock is resistant to stress. Fibres grow in a very narrow crack because the limited growth competition is only compatible with growth on an essentially closed surface (Hilgers & Urai 2002). The growth zonation is highlighted by colour zonation of calcite and sometimes by the presence of fluid inclusions in calcite. Minor deformation of the veins has occurred either during vein growth or after vein growth as vein calcite is twinned on the edge of the vein. Moreover, the movements during vein formation are indicated by slightly curved calcite fibres containing minor mechanical twins showing signs of tectonic deformation (Ramsay & Huber 1983).

Fibre curvature, growth direction and the type of host rock vs. vein composition are consistent with unitaxial syntaxial growth at the vein-wall interface (Durney & Ramsay 1973; Ramsay & Huber 1983; Passchier & Trouw 1996). This is also supported by the microstructure of the polymineral tension vein, where growth is in one direction only at a single unitaxial growth plane between vein and wall rock (Durney & Ramsay 1973; Urai et al. 1991; Hilgers et al. 2001; Hilgers & Urai 2002). The direction of growth is indicated by the increasing width of the fibres towards the vein wall. Generally, both fibrous marginal zones do not differ in the direction of growth of calcite fibres.

Similarly, syntectonic fibrous veins tend to have a narrow quartz selvage (Elburg et al. 2002; Hilgers & Urai 2002), consisting of small quartz crystals that grew out from the wall rock (syntaxial growth) which is consistent with our observation. The width of this selvage is quite independent of the width of the vein.

*Median zone.* The difference in texture indicates that crystal growth inside the median zone was driven by a different mechanism than the growth of the fibrous zones on both margins of the vein (Bons & Montenari 2005). The shape of grains (elongated-blocky) shows that growth competition was not suppressed during the precipitation of calcite. This is indicated by the fact that the fracture was very narrow and had a rough surface (Urai et al. 1991). The thickness of the central zone of fracture (now formed by granular calcite) initiated after the fibrous stage of development was probably not less than 10 mm (Hilgers & Urai 2002). This assumption is supported by the constant width of the central parts of veins (about 1 cm). Solid inclusions (angular fragments of

surrounding rocks) are irregularly enclosed in calcite and do not define any median growth plane of calcite grains. This observation may indicate that fragments of surrounding rock formed during initial opening of the crack.

### *P-T conditions of crystallization*

Constant liquid-vapour ratios in primary L + V fluid inclusions in calcite suggest trapping of the homogeneous fluid phase. Therefore, the measured homogenization temperatures are the minimum possible formation temperatures (Goldstein & Reynolds 1994). The true trapping temperatures and pressures can be specified only if independent temperature and/or pressure estimates are available. Since the aggregates of chlorite enclosed in both granular and fibrous calcite from V2 vein show very high Si values often exceeding the theoretical maximum of 4 apfu, chlorite compositional geothermometers (Cathelineau 1988; Jowett 1991) can not be used for determining the temperature of their formation.

However, as an upper possible temperature limit for syntectonic V2 veins can be used the regional burial temperature maximum (ca. 160 °C) indicated by vitrinite reflectance data, illite crystallinity, and fluid inclusions (Botor et al. 2006). The calculations show that these veins were probably formed in low-pressure conditions (< 1 kbar; Fig. 8). The wide range of Th values observed for fibrous calcite may be
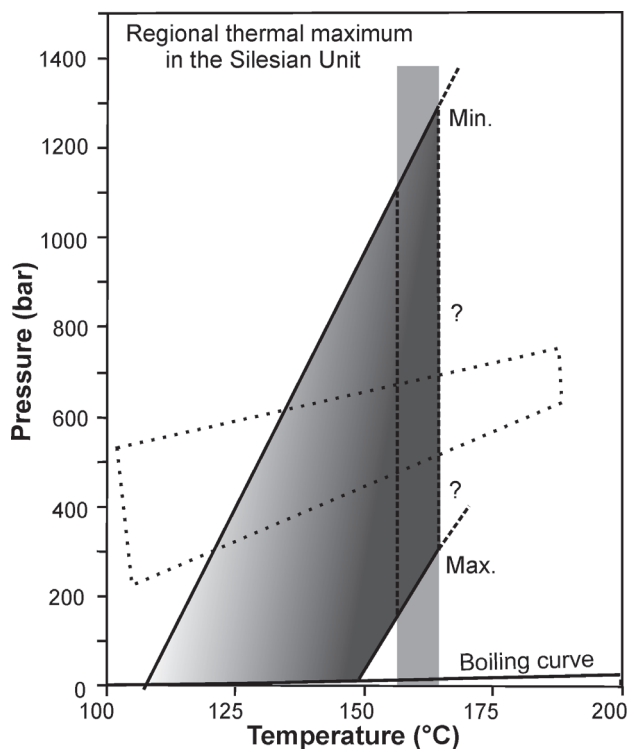
due to variations in pressure which typically fluctuates between lithostatic and hydrostatic one during formation of the crack-seal veins (Hurai et al. 2002). We can assume a decrease of temperature of parent solution during precipitation of granular calcite from the V2 vein.

### *Salinity of fluids*

The Th-salinity plot (Fig. 6c) documents mixing of two fluid endmembers which differ in temperature and salinity for calcite V. The presence of seawater in the fluid mixture could be deduced from the upper limit of the fluid salinity close to the seawater value of 3.5 wt. %. We assume that seawater retained in pore system of sandstones and could be released later into the cracks. The low-salinity fluid endmember can be the diagenetic solutions derived from dehydration of clay minerals. In the given geological setting the activity of such low-salinity waters has been documented in clay-rich sedimentary sequences (cf. Polách et al. 2008; Dolníček & Polách 2009). The high Si content, Fe-depletion, and Al/(Al + Mg + Fe) values greater than 0.35 in chlorite from Jasenice may also be explained by the crystallization from solutions derived from argillaceous rock in the reducing conditions (Zhang et al. 2008).

### *Trace element signature of hydrothermal fluid*

The low contents of elements incompatible with calcite structure (e.g. Ga, Zr, Rb) indicate a negligible contamination of calcites by the host rock and/or vein silicate mineral phases. High content of Sr (1100 ppm) in calcite samples can be explained by its high mobility during the hydrothermal process and co-precipitation with Ca-minerals. The observed lower content of Sr in granular calcite from the V2 vein (983 ppm) can probably be related to the gradual cooling of the hydrothermal solution and decrease of the rock/water ratio during the later stage of development of the vein (Dickin et al. 1984).

The low concentrations of REE in calcite from the tension vein suggest relatively rapid precipitation of calcite (Möller et al. 1997). The chondrite-normalized REE patterns (Fig. 6) follow similar trends in all samples (host rock and vein calcite) characterized by systematic decrease from La to Lu with the exception of Ce and Eu, which are sensitive to Eh changes  (Lee et al. 2003; Dolníček 2005). The LREE enrichment of calcite similar to host rock indicates the low content of strong REE-complexing ligands (F⁻, OH⁻ or $CO_3^{2-}$) in the hydrothermal solution and suggests that especially sorption processes played a significant role during incorporation of REE into calcite (Guy et al. 1999; Lee et al. 2003). It also shows local REE source without fractionation. The low content of strong REE-complexing ligands would be compatible with dehydration-related fluids originating by dewatering of clay minerals (Bau & Möller 1992) during diagenesis. These solutions mixed with residual marine waters and were passed through the body of igneous rocks along the pressure gradient. When a fluid is percolated through the teschenite, the REE-complexing ligands (e.g. F and P) released by breakdown of magmatogenic mineral phases were contin-



**Fig. 8.** Interpretation of P-T conditions for syntectonic veins at the Jasenice site and comparison with other mineralizations in the Silesian Unit hosted by teschenite rock series (Dolníček et al. 2012 — dotted line). The regional thermal maximum is from Botor et al. (2006). The representative utmost isochores (solid lines — outliers neglected) shown have been calculated using the computer program Flincor (Brown 1989) with equation of state by Zhang & Frantz (1987).

uously removed and their concentration in the fluid phase remains low (Dolníček et al. 2010a).

The negative Ce-anomaly observed in fibrous calcite can indicate a seawater component in the fluid (Hecht et al. 1999; Wamada et al. 2007). Alternatively, the presence of both negative Ce-anomaly and positive Eu-anomaly found in granular calcite from median of composite vein suggest the mixing of several types of fluids which were formed under various redox conditions (Möller et al. 1991). A positive Eu-anomaly in the middle part of a composite vein can be explained either by decrease of temperature of the solution under 200 °C or due to change of Eh in a hydrothermal solution (Bau & Möller 1992). Although the observed Th values do not correspond to high-temperature conditions, we potentially can not exclude a short-term activity of tectonically generated overheated fluids in this geological situation (cf. Dolníček et al. 2012). Nevertheless the absence of a positive Yb anomaly (Yb/Yb* = 0.9) (Bau & Möller 1992) combined with the presence of a negative Ce-anomaly can indicate a lower temperature of the parent solution during precipitation of granular calcite from the V2 vein (Wood 1990; Bau & Möller 1992; Barker et al. 2006).

### $\delta^{18}O$ and $\delta^{13}C$ of the hydrothermal fluid

The fluid $\delta^{18}O$ and $\delta^{13}C$ characteristics have been calculated from mineral $\delta^{18}O$ and $\delta^{13}C$ data and homogenization temperatures measured in the respective samples (Table 2). The calculated fluid $\delta^{18}O$ values ranging from +1.7 to +9.0 ‰ SMOW are similar for all growth zones of the fibrous calcite. The granular calcite from the median shows more positive fluid $\delta^{18}O$ values between +5.0 and +12.5 ‰ SMOW. The fluid $\delta^{13}C$ values show a narrower range from –14.1 to –13.0 ‰ PDB for fibrous calcite and –12.0 to –11.8 ‰ PDB for granular calcite. The calcite from a younger granular vein yielded ranges of +0.2 to +3.4 ‰ SMOW and –13.1 to –12.7 ‰ PDB for fluid $\delta^{18}O$ and $\delta^{13}C$, respectively. It should be noted that the use of pressure-uncorrected Th values leads to underestimated fluid $\delta^{13}C$ and especially $\delta^{18}O$ values for syntectonic calcites. However, the qualitative interpretation of the source of their fluids (see below) will not be affected.

The variable $\delta^{18}O$ values may be compatible with mixing of two (or more) fluids with contrasting isotope compositions (e.g. residual seawater residing in the pore system of sandstones with a near-zero $\delta^{18}O$ value (Sheppard 1986) could mix with water characterized by highly positive $\delta^{18}O$ values. In the given geological setting, the diagenetic waters, derived from surrounding sedimentary rocks, thus probably represent the best candidate to explain both the low fluid salinity and elevated $\delta^{18}O$ values. The observed elevated $\delta^{18}O$ values in a paragenetically younger granular calcite of composite vein (V2) could be explained by a pronounced isotopic exchange of oxygen between rocks and fluid phase (Sheppard 1986; Torres-Alvarado et al. 2011). Last but not least the generally high $\delta^{18}O$ values of fluids may also originate during interaction of fluids with isotopically heavy sedimentary carbonates (Dolníček et al. 2010a). The lower $\delta^{18}O$ values of the fluids in the youngest phases (V1 veins) can be

explained by either decreasing temperature of the fluid-rock interaction or mixing with isotopically light surface waters (i.e. meteoric or marine water) in the latest stage of the mineralizing process (Sheppard 1986). The calculated $\delta^{13}C$ values of the fluid phase indicate a mixed carbon source, most likely from both "carbon of the homogenized Earth's crust" ($\delta^{13}C = -5$ to –8 ‰ PDB) averaged from various crustal sources during fluid evolution and carbon derived from oxidized organic matter ($\delta^{13}C = -20$ to –30 ‰ PDB). The negligible variations in fluid $\delta^{13}C$ values can be explained by rock-buffered fluid system (Hoefs 1997).

### Comparison with other hydrothermal systems

The available data on fluid salinity from Jasenice are comparable to those from previously studied hydrothermal mineralizations in the Silesian Unit (Fig. 6c). Most post-magmatic mineral associations were formed from low-temperature (<50 to 170 °C) and low-salinity (0.0 to 4.5 wt. % NaCl equiv.) fluids (Polách 2008; Urubek & Dolníček 2008, 2011; Urubek 2009; Dolníček et al. 2010a,b, 2012). The only exception is early post-magmatic stage which was formed from high-temperature (390–510 °C) and high-salinity (47–57 wt. % salts) fluids released during crystallization of magma (Dolníček et al. 2010a). The hydrothermal veins hosted by sedimentary rocks formed from low-temperature (mostly 60–155 °C, exceptionally up to 220 °C) and low-salinity (1.0-3.6 wt. % NaCl eq.) fluids (Świerczewska et al. 2000; Polách 2008; Polách et al. 2008; Dolníček &
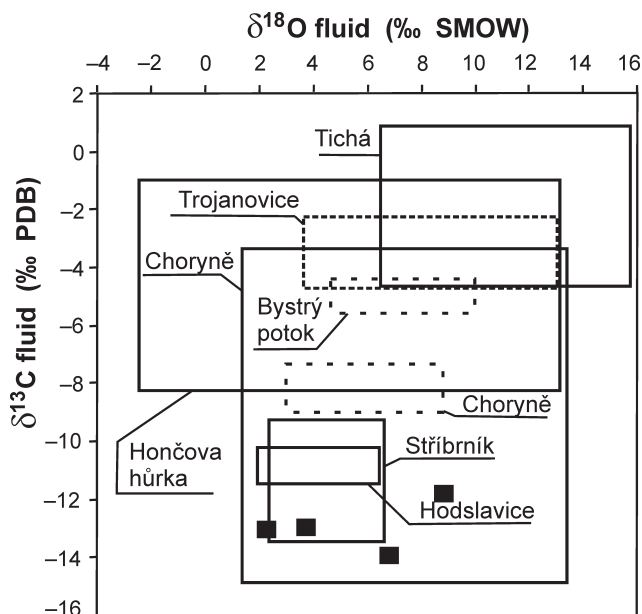


**Fig. 9.** Oxygen and carbon isotopic composition of hydrothermal fluids from Jasenice (data points) in comparison with other localities in the Silesian Unit (outlined; full line — veins hosted by igneous rocks; dashed line — veins hosted by sedimentary rocks; coarsely dashed line — diagenetic veins; thin dashed line — postectonic veins). The comparative data are from Polách (2008), Urubek & Dolníček (2008), Dolníček & Polách (2009), Urubek (2009), and Dolníček et al. (2010a,b, 2012).

Polách 2009; Jarmolowicz-Szulc et al. 2012). The studied syntectonic veins show slightly lower fluid $\delta^{13}C$ values in comparison with other veins in the studied area, while the range of $\delta^{18}O$ values is almost identical (Fig. 9). This observation indicates that carbon originating from either earlier (i.e. post-magmatic) mineralizations and/or from organic matter participated in formation of the syntectonic veins. The REE patterns of hydrothermal vein carbonates are similar to the other carbonate-bearing mineralizations in the Silesian Unit (Fig. 7). Recycling of at least some components from earlier mineralizations confirm the rock-buffered nature of the hydrothermal system during syntectonic veining.

## Conclusion

Hydrothermal mineralization from the locality of Jasenice is located in an outcrop of picrite in two morphologic types: (i) granular veins without preferred spatial orientation and (ii) composite unitaxial syntaxial syntectonic veins. Granular veins 0.2 to 2 cm thick are composed only of isometric grains of calcite. The composite tension vein is asymmetrically banded. It is composed mainly of calcite and minor chlorite (pennine), quartz, and pyrite. The vein was formed by two mechanisms. The peripheral fibrous parts are the result of episodic hydraulic fracturing followed by the healing of the microfractures by calcite (crack-seal mechanism) resulting in a fibrous texture. By contrast, the middle part of the composite vein composed of granular calcite originated in a brittle regime, when fluids most likely moved along a fracture in a pre-existing vein.

Generation of the parent fluids is probably connected with Tertiary deformation, folding and thrusting of the whole Silesian Unit. The fluids were derived by mixing of seawater residing in pores of clastic sediments and diagenetic waters produced by dewatering of clay minerals in associated flysch sediments. The REE and isotopic studies suggest the existence of a geochemically more or less closed system buffered by the host rock sequence. The fluid movement was mainly driven by the tectonic suction pump which continuously supplied ions into the fluid. The vein-forming components were transported mainly by diffusion to their deposition site (Sibson et al. 1975). Similarly, fibrous crystals growing in small cracks (due to prevention of the growth of competition) do not favour large-scale fluid conduits. It is more likely that they indicate pervasive flow or diffusion (Bons 2000; Oliver & Bons 2001; Elburg et al. 2002).

Hydrothermal minerals precipitated from low-salinity (0.4 to 3.4 wt. % NaCl eq.) and low-temperature (Th = 66 to 163 °C) aqueous solutions. The REE data indicate that the fluid was poor in strong REE-complexing ligands and that redox potential changed during crystallization.

The above described interpretations of fluid origin are comparable to the results obtained from other types of hydrothermal mineralization hosted by teschenite rock series in the Silesian unit as well as those hosted by flysch sediments implying similar sources of hydrothermal solutions in both environments. The existing data moreover suggest a continuous evolution of the fluid system in the given area from sedi-

mentation and post-magmatic alteration of associated teschenite intrusions through diagenesis, rock deformation during the Alpine Orogeny, up to the post-orogenic faulting.

## References

Anders E. & Grevesse N. 1989: Abundances of the elements: meteoritic and solar. *Geochim. Cosmochim. Acta* 53, 197–214.

Barker S.L.L., Cox S.F., Eggins S.M. & Gagan M.K. 2006: Microchemical evidence for episodic growth of antitaxial veins during fracture-controll fluid flow. *Earth Planet. Sci. Lett.* 250, 331–344.

Bau M. & Möller P. 1992: Rare earth element fractionation in metamorphogenic hydrothermal calcite, magnesite and siderite. *Miner. Petrology* 45, 231–246.

Bodnar R.J. 1993: Revised equation and table for determining the freezing point depression of $H_2O$ NaCl solutions. *Geochim. Cosmochim. Acta* 57, 683–684.

Bons P.D. 2000: The formation of veins and their microstructures. *J. Virtual Explorer 2.* on-line — http://virtualexplorer.com.au/special/meansvolume/contribs/bons/

Bons P.D. & Montenari M. 2005: The formation of antitaxial calcite veins with well-developed fibres, Oppaminda Creek, South Australia. *J. Struct. Geol.* 27, 231–248.

Botor D., Dunkl I., Rauch-Wlodarska M. & von Eynatten H. 2006: Attempt to dating of accretion in the West Carpathian Flysch Belt: apatite fission track thermochronology of tuff layers. *Geolines* 20, 21–23.

Brown Ph.E. 1989: FLINCOR; a microcomputer program for the reduction and investigation of fluid-inclusion data. *Amer. Mineralogist* 74, 1390–1393.

Cathelineau M. 1988: Cation site occupancy in chlorites and illites as a function of temperature. *Clay Miner.* 23, 471–485.

Cosgrove J.W. 1993: The interplay between fluids, folds and thrusts during the deformation of a sedimentary succession. *J. Struct. Geol.* 15, 491–500.

Deines P., Langmuir D. & Harmon R.S. 1974: Stable carbon isotope ratios and the existence of a gas phase in the evolution of carbonate ground waters. *Geochim. Cosmochim. Acta* 38, 1147–1164.

Dickin A.P., Henderson C.M.B. & Gibb F.G.F. 1984: Hydrothermal Sr contamination of the Dippin sill, Isle of Arran, Western Scotland. *Mineral. Mag.* 48, 311–322.

Dolníček Z. 2005: Cenozoic fluorite mineralization from the Brunovistulicum, southeastern margin of the Bohemian massif (Czech Republic). *Geol. Carpathica* 56, 2, 169–177.

Dolníček Z. & Polách M. 2009: Hydrothermal mineralization in sandstones of Variegated Godula Member at the locality Bystrý potok (Moravskoslezské Beskydy Mts.). *Acta Mus. Morav., Sci. Geol.* 94, 97–110 (in Czech).

Dolníček Z., Kropáč K., Uher P. & Polách M. 2010a: Mineralogical and geochemical evidence for multi-stage origin of mineral veins hosted by teschenites at Tichá, Outer Western Carpathians, Czech Republic. *Chem. Erde* 70, 267–282.

Dolníček Z., Urubek T. & Kropáč K. 2010b: Post-magmatic hydrothermal mineralization associated with Cretaceous picrite

(Outer Western Carpathians, Czech Republic): interaction between host rock and externally derived fluid. *Geol. Carpathica* 61, 327–339.

Dolníček Z., Kropáč K., Janíčková K. & Urubek T. 2012: Diagenetic source of fluids causing the hydrothermal alteration of teschenites in the Silesian Unit, Outer Western Carpathians, Czech Republic: Petroleum-bearing vein mineralization from the Stříbrník site. *Mar. Petrol. Geol.* 37, 27–40.

Dostal J. & Owen J.V. 1998: Cretaceous alkaline lamprophyres from northeastern Czech Republic: geochemistry and petrogenesis. *Geol. Rdsch.* 87, 67–77.

Durney D.W. & Ramsay J.G. 1973: Incremental strains measured by syntectonic crystal growths. *Gravity and Tectonics*, 67–96.

Elburg M.A., Bons P.D., Foden J. & Passchier C.W. 2002: The origin of fibrous veins: constraints from geochemistry. *Geol. Soc., London, Spec. Publ.* 200, 103–118.

Eliáš M. 1970: Lithology and sedimentology of the Silesian Unit in the Moravskoslezské Beskydy Mts. *Sborn. Geol. Věd, Geol.* 18, 7–99 (in Czech).

Födör L. 1991: Evolution tectonique et paleo-champs de contraintes oligocenes a quaternaires de la zone de transitiv Alpes orientales-Carpathes occidentales: formativ et developpment des bassins de Vienne at Nord-panonnies. *MSc. Thesis*, Paris, 1–77.

Goldstein R.H. & Reynolds T.J. 1994: Systematics of fluid inclusions in diagenetic minerals. *Soc. Sed. Geol., Short Course* 31, 1–199.

Golonka J., Oszypko N. & Ślaczka A. 2000: Late Carboniferous — Neogene geodynamic evolution and paleogeography of the circum-Carpathian region and adjacent areas. *Ann. Soc. Geol. Pol.* 70, 107–136.

Guy C., Daux V. & Schott J. 1999: Behaviour of rare earth elements during seawater/basalt interactions in the Mururoa Massif. *Chem. Geol.* 158, 21–35.

Havíř J. 2000: Study of orientations of principal paleostress in the wider area of the Moravian Gate and Pálava. *MSc. Thesis, PřF MU Brno*, 1–89 (in Czech).

Hecht L., Freiberger R., Gilg H.A., Grundmann G. & Kostitsyn Y.A. 1999: Rare earth element and isotope (C, O, Sr) characteristics of hydrothermal carbonates: genetic implications for dolomite-hosted talc mineralization at Gopfersgrun (Fichtelgebirge, Germany). *Chem. Geol.* 155, 1, 115–130.

Hilgers C. & Sindern S. 2005: Textural and isotopic evidence on the fluid source and transportmechanism of antitaxial fibrous microstructures from the Alps and the Appalachians. *Geofluids* 5, 239–250.

Hilgers C. & Urai J.L. 2002: Microstructural observations on natural syntectonic fibrous veins: implications for the growth process. *Tectonophysics* 352, 257–74.

Hilgers C., Dilg-Gruschinski K. & Urai J.L. 2004: Microstructural evolution of syntaxial veins formed by advective flow. *Geology* 32, 261–4.

Hilgers C., Koehn D., Bons P.D. & Urai J.L. 2001: Development of crystal morphology during uniitaxial growth in a progressively opening fracture. II. Numerical simulations of the evolution of antitaxial fibrous veins. *J. Struct. Geol.* 23, 873-885.

Hoefs J. 1997: Stable isotope geochemistry, 4th edition. *Springer–Verlag*, Berlin, New York, 1–244.

Hovorka D. & Spišiak J. 1988: Mesozoic volcanism in the Western Carpathians. *Veda*, Bratislava, 1–263 (in Slovak).

Hurai V., Kihle J., Kotulová J., Marko F. & Świerczewska A. 2002: Origin of methane in quartz crystals from the Tertiary accretionary wedge and fore-arc basin of the Western Carpathians. *Appl. Geochem.* 17, 1259–1271.

Jarmolowicz-Szulc K., Karwowski L. & Marynowski L. 2012: Fluid circulation and formation of minerals and bitumens in the sedimentary rocks of the Outer Carpathians — based on studies on the quartz-calcite-organic matter association. *Mar. Petrol. Geol.* 32, 138–158.

Jowett E.C. 1991: Fitting iron and magnesium into the hydrothermal chlorite geothermometer. In: *GAC/MAC/SEG Joint Annual Meeting, Program with Abstracts*, Toronto, pp. A62.

Kropáč K., Buriánek D. & Zimák J. 2012: Origin and metamorphic evolution of Fe-Mn-rich garnetites (coticules) in the Desná Unit (Silesicum, NE Bohemian Massif). *Chem. Erde* 72, 219–236.

Kudělásková J. 1987: Petrology and geochemistry of selected rock types of teschenite association, (Outer Western Carpathians). *Geol. Carpathica* 38, 545–573.

Lee S.G., Lee D.H., Kim Y., Chae B.G., Kim W.Y. & Woo N.Ch. 2003: Rare earth elements as indicators of groundwater environment changes in a fractured rock system: evidence from fracture-filling calcite. *Appl. Geoch.* 18, 135–143.

Lucińska-Anczkiewicz A., Villa I.M., Anczkiewicz R. & Ślaczka A. 2002: $^{40}Ar/^{39}Ar$ dating of alkaline lamprophyres from the Polish Western Carpathians. *Geol. Carpathica* 53, 45–52.

McCrea J.M. 1950: On the isotopic chemistry of carbonates and a palaeotemperature scale. *J. Chem. Phys.* 18, 849–857.

McLennan S.M. 1989: Rare earth elements in sedimentary rocks: influence of prohnance and sedimentary processes. *Rev. in Mineralogy* 21, 169–200.

Melka K. 1965: A proposal of classification of chlorite minerals. *Věst. Ústř. Úst. Geol.* 40, 23–27 (in Czech).

Milovský R. & Hurai V. 2003: P-T parameters and immiscibility phenomena in synkinematic fluids of the thin-skinned Muráň nappe (Western Carpathians). In: Dégi J. & Szabó Cs. (Eds.): XVIIth European Current Research on Fluid Inclusions, Budapest (Hungary), June 5–7, 2003. *Acta Univ. Szeged., Abstract Series* 2, 123–124.

Milovský R., Hurai V., Plašienka D. & Biroň A. 2003: Hydrotectonic regime at soles of overthrust sheets: textural and fluid inclusion evidence from basal cataclasites of the Muráň nappe (Western Carpathians, Slovakia). *Geodinam. Acta* 16, 1–20.

Mlynář A. 2000: Tectonics of selected parts of the Carpathian Flysch in north Moravia. *MSc. Thesis, PřF MU*, Brno, 1–81 (in Czech).

Monecke T., Kempe U., Monecke J., Sala M. & Wolf D. 2002: Tetrad effect in rare earth element distribution patterns: a method of quantification with application to rock and mineral samples from granite-related rare metal deposits. *Geochim. Cosmochim. Acta* 66, 1185–1196.

Möller P., Stober I. & Dulski P. 1997: Seltenerdelement-, Yttrium-Gehalte und Bleiisotope in Thermal- und Mineralwässern des Schwarzwaldes. *Grundwasser* 3, 118–131.

Möller P., Lüders V., Schroder J. & Luck J. 1991: Element partitioning calcite as a function of solution flow rate: a study on vein calcites from the Harz Mountains. *Mineralium Depos.* 26, 175–179.

Oliver N.H.S. & Bons P.D. 2001: Mechanisms of fluid flow and fluidrock interaction in fossil metamorphic hydrothermal systems inferred from vein-wall rock patterns, geometry and microstructure. *Geofluids* 1, 137–162.

O'Neil J.R., Clayton R.N. & Mayeda T.K. 1969: Oxygen isotope fractionation in divalent metal carbonates. *J. Chem. Phys.* 51, 5547-5558.

Pacák O. 1926: Volcanic rocks at the northern footwall of the Moravské Beskydy Mts. *Rozpr. Českosl. Akad. Věd Umění,* 1–35 (in Czech).

Passchier C.W. & Trouw R.A.J. 1996: Microtectonics. *Springer–Verlag*, Berlin, 1–289.

Plašienka D., Grecula P., Putiš M., Kováč M. & Hovorka D. 1997: Evolution and structure of Western Carpathians: an overview. *Miner. Slovaca–Monograph*, Bratislava, 1–24.

Polách M. 2008: Hydrothermal mineralization in the eastern part of

the Moravskoslezské Beskydy Mts. (Outer West Carpathians). *MSc. Thesis*, UP Olomouc, 1–72 (in Czech).

Polách M., Dolníček Z. & Malý K. 2008: Hydrothermal mineralization at the locality Pindula near Frenštát pod Radhoštěm (Silesian unit, Outer West Carpathians). *Acta Mus. Morav., Sci. Geol.* 93, 127–135 (in Czech).

Ramsay J.G. 1980: The crack-seal mechanism of rock deformatiom. *Nature* 284, 135–139.

Ramsay J.G. & Huber M.I. 1983: The techniques of modern structural geology. *Academic Press*, London, 248–251.

Roedder E. 1984: Fluid inclusions. *Rev. in Mineralogy* 12, 1–644.

Sheppard S.M.F. 1986: Characterization and isotopic variations in natural waters. *Rev. in Mineralogy* 16, 165–183.

Shepherd T.J., Rankin A.H. & Alderton D.H.M. 1985: A practical guide to fluid inclusion studies. *Blackie*, Glasgow and London, 1–239.

Sibson R.H., McMoore J. & Rankin A.H. 1975: Seismic pumping — a hydrothermal fluid transport mechanism. *J. Geol. Soc., London* 131, 653–659.

Spišiak J. & Mikuš T. 2008: Ba and Sr rich mineral phases in the Cretaceous volcanites; Western Carpathians. In: Geochémia 2008 proceedings. *ŠGÚDŠ*, Bratislava, 54–56 (in Slovak).

Stráník Z., Menčík E., Eliáš M. & Adámek J. 1993: Flysch belt of the Western Carpathians, autochthonous Mesozoic and Paleogene in Moravia and Silesia. In: Přichystal A., Obstová V. & Suk M. (Eds.): Geology of Moravia and Silesia. *PřF MU Brno*, 59–70 (in Czech).

Szczesny R. 2003: Reconstruction of stress directions in the Magura and Silesian Nappes (Polish Outer Carpathians) based on analysis of regional folds. *Geol. Quart.* 47, 3, 289–298.

Świerczewska A., Tokarski A.K. & Hurai V. 2000: Joints and mineral veins during structural evolution: case study from the Outer Carpathians (Poland). *Geol. Quart.* 44, 3, 333–339.

Šmíd B. 1962: An overview of geology and petrography of rocks of teschenite association from the northern footwall of the Beskydy Mts. *Geol. Práce* 63, 53–60 (in Czech).

Torres-Alvarado I.S., Satir M., Pérez-Zárate D. & Birkle P. 2011: Stable isotope composition of hydrothermally altered rocks and hydrothermal minerals at the Los Azufres geothermal field, Mexico. *Turk. J. Earth Sci.* 21, 127–143.

Urai J.L., Williams P.F. & Roermund H.L.M. 1991: Kinematics of crystal growth in syntectonic fibrous veins. *J. Struct. Geol.* 13, 823–836.

Urubek T. 2006: Hydrothermal mineralization in western part of the Moravskoslezské Beskydy Mts. (Outer Western Carpathians). *Bc. Thesis, UP Olomouc*, 1–38 (in Czech).

Urubek T. 2009: Hydrothermal mineralization in western part of the Silesian Unit (Outer Western Carpathians): genetic aspects. *MSc. Thesis, UP Olomouc*, 1–87 (in Czech).

Urubek T. & Dolníček Z. 2008: Hydrothermal mineralization in rocks of teschenite association from Hodslavice near Nový Jičín (Silesian unit, Outer West Carpathians). *Čas. Slez. Muz. Opava (A)* 57, 21–30 (in Czech).

Urubek T. & Dolníček Z. 2011: Hydrothermal mineralisation in rock of teschenite association near Nový Jičín (Silesian Unit, Outer Western Carpathians). *Geol. Výzk. Mor. Slez.* 17, 83–86 (in Czech).

Urubek T., Dolníček Z. & Uhlíř D. 2009: Mineralogy and formation conditions of the hydrothermal mineralization in picrite from Choryně near Valašské Meziříčí (Silesian Unit, Outer Western Carpathians). *Čas. Slez. Muz. Opava (A)* 58, 175–190 (in Czech).

Warmada W.I., Lehmann B., Simandjuntak M. & Hemes H.S. 2007: Fluid inclusion, rare-earth element and stable isotope study of carbonate minerals from the Pongkor epithermal gold–silver deposit, West Java, Indonesia. *Res. Geol.* 57, 2, 124–135.

Wood S.A. 1990: The aqueous geochemistry of the rare-earth elements and yttrium. 2. Theoretical predictions of speciation in hydrothermal solutions to 350 °C at saturation water vapor pressure. *Chem. Geol.* 88, 99–125.

Zhang Y.G. & Frantz J.D. 1987: Determination of the homogenization temperatures and densities of supercritical fluids in the system $NaCl-KCl-CaCl_2-H_2O$ using synthetic fluid inclusions. *Chem. Geol.* 64, 335–350.

Zhang Z., Liu S. & Wu J. 2008: Characteristic and the formation conditions of chlorite in Xiazhuang uranium ore-field, South China. *Goldschmidt Conference Abstracts A1092. Cambridge*, United Kingdom, 1–1143.